ARTICLE

Temperature and pressure in the environment of epithermal alteration: a case study at Ibaré Lineament, Rio Grande do Sul, Brazil

Kelvyn Mikael Vaccari Ruppel[1]* ⓘD, Norberto Dani[1],
Marcus Vinicius Dorneles Remus[1] ⓘD, Luiz Henrique Ronchi[2] ⓘD,
Marcia Elisa Boscato Gomes[1], Eliel Senhorinho[3] ⓘD

ABSTRACT: *The Ibaré Lineament is a shear zone that sections the Western portion of Sul-riograndense Shield, affecting the orthogneissic rocks of Santa Maria Chico Granulitic Complex, acting as a conduct for hydrothermal fluids. The studied hydrothermal mineralogy reflects a propylitic alteration paragenesis that is composed of Fe-clinochlore, epidote, albite, calcite and quartz, typical low-pressure paragenesis (< 2,000 bar). This mineral association reflects an equilibrium in a neutral to slightly alkaline pH. Using the new approach for chlorite geothermometry, an average formation temperature of 274°C was obtained, compatible with the stability of polytype IIb chlorite and with the irregular textures of twinning in calcites. The fluid inclusions in quartz establish a low-salinity system (2.45 wt.% NaCl eq.) and an average temperature of 175°C. The obtained temperatures are interpreted as a continuum cooling model with meteoric fluids entrance. The system pressure is evaluated from isochores, reaching an average value of 1,560 bar. This is the first temperature and pressure estimate to the Ibaré Shear Zone, which enabled the establishment of a shallow hydrothermal system (epithermal) with fluid interaction from magmatic and meteoric sources, confirmed by the behavior of carbon and oxygen stable isotopes, which indicated an the origin from mixed sources.*

KEYWORDS: *Ibaré Lineament; Chloritization; Epithermal; Propylitic alteration; Geothermobarometry.*

INTRODUCTION

The Ibaré Lineament is in the Western sector of Sul-riograndense shield as a NW-SE-oriented geostructure on the limit between Taquarembó (SW) and São Gabriel (NE) terranes. It is the superficial expression of a subvertical brittle-ductile transcurrent shear zone, initially with dextral sense, which was late reactivated in successive episodes with sinistral kinematic at shallow crustal levels (Luzardo & Fernandes 1990, Fernandes *et al.* 1992, Ruppel 2010, Laux 2017). Such lineament (Jost & Hartmann 1984, Naumann *et al.* 1984), first named as Suspiro Linhares Fault (Ribeiro 1978), will be called in the present paper as Ibaré Shear Zone (ISZ'). It has an overall Northwest direction that constitutes a fault system affecting rocks in an extent of about 10 km of average width.

The ISZ created space and conditions for the fluid percolation (Senhorinho 2012), which interacted with Paleoproterozoic rocks of Santa Maria Chico Granulitic Complex (SMCGC) and younger rocks, such as Brasiliano granitoids (Iglesias 2000, Goulart 2014). Reports about the identification of free gold spots around the region, identified in active current sediments (Toniolo & Kirchner 1995, 2000), turn the ISZ into a prospect for mineralizations associated with hydrothermal events. Driven by the economic potential, a study was developed with techniques to better evaluate the pressure and temperature (P-T) conditions of the hydrothermal alteration in a specific sector of the ISZ, composed by orthogneissic rocks of the SMCGC. In the shear zone, an intense process of chloritization could be identified, which was sampled in details with the aim to determine, with specific tools, the pressure and temperature of the fluids. The P-T conditions and the

source of fluids are evaluated through information obtained by the alteration mineralogy, chlorite analysis with the study of fluid inclusions (FIs) in quartz veins and with the behavior of C and O isotopes in associated carbonates.

STUDY AREA GEOLOGY

In Southwestern Rio Grande do Sul state, the ISZ separates the West part of the Sul-riograndense Shield in two terranes, Taquarembó and São Gabriel (Fig. 1A). The Western domain of Taquarembó Terrane is interpreted as belonging to Río de La Plata Craton and is composed by metamorphic rocks of the SMCGC (Nardi & Hartmann 1979, Chemale Jr. 2000). The SMCGC occupies the Southeast portion of the Sul-riograndense Shield in an area of about 600 km² (Hartmann 1998), being limited on its Northeast portion by the São Gabriel Terrane and ISZ rocks (Fig. 1B).

The SMCGC rocks vary from isotropic to banded, containing foldings and foliation predominantly of NW direction with high dip. The associations contained on the SMCGC

are divided into three groups: mafic to ultramafic granulites, orthogneisses and paragneisses (Hartmann 1987, 1991, 1998, Philipp *et al.* 2017). The protoliths are interpreted as a TTG association formed in an island of environment or continental margin (Laux & Bongiolo 2011, Philipp *et al.* 2017), with Neoarchean ages of about 2.55 Ga (Hartmann *et al.* 2008), subjected to regional metamorphism of granulite facies at 2.1 Ga in conditions of 700–850°C and 5 to 10 kb (Hartmann 1987, 1991, 1998). Later, the SMCGC (Fig. 1B) was affected by the intrusion of Brasiliano granites (Hartmann 1987), which created effects of retrometamorphism and reworking of the ISZ and, additionally, by carbonatites recently identified in the region (Cerva-Alves *et al.* 2017). In this study, only the orthogneisses were contemplated.

MATERIALS AND METHODS

Non- to deeply-chloritized orthogneisses samples were collected at a section along the railroad at the location of Três Estradas, in the town of Lavras do Sul-RS (Fig. 1B). The thin
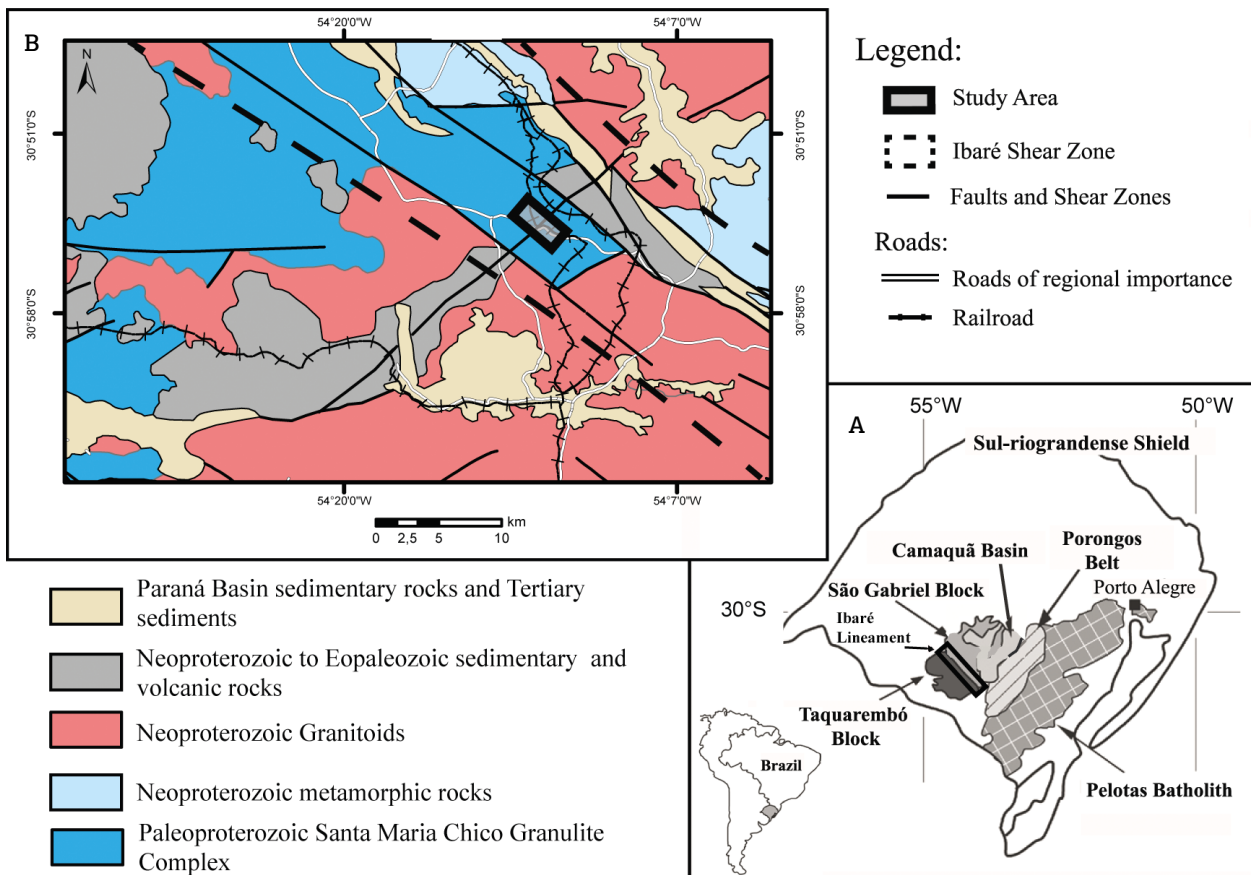

Figure 1. Geo-structural map of the study area. (A) Structural compartments of the Sul-riograndense Shield and location of the Ibaré Shear Zone (ISZ) with NW orientation in the limit between São Gabriel and Taquarembó terranes. (B) Localization of the study area inside the ISZ range and general geologic context. Modified from Wildner (2006) and Gastal & Ferreira (2013).

section description was made with the assistance of an optical microscope model (Leica-DM4500 P LED). The optical images were obtained with the same microscope, using the digital camera Leica Model DFC-495. For the analysis of FIs, thick bipolished sections were used, proceeding to the analysis at the Fluid Inclusion Laboratory of the Geological Engineering course at the Federal University of Pelotas (UFPel), with the Linkam THMSG600 equipment for heating and freezing, attached to a Nikon 50i microscope. The equipment calibration was made with a synthetic aquo-carbonic fluid inclusion (-56.6°C *synth.*, FIs), demineralized water (0.0°C) and products with a known fusion point, such as sodium nitrate (308°C) and potassium dichromate (398°C). To have more precise measurements and lower the effects of metastability, the analysis was made with low-heating rates (0.5 to 3 °C/min) at the temperature ranges near the phase transitions; therefore, obtaining a precision of ± 0.1°C. The salinity of the FIs was determined according to Bodnar (2003). Other physical and chemical properties of the fluids were calculated with the AqSo1e™ software, and the isochores were calculated using the ISOC™ software, both joining the software package used for computational FIs modelling of Bakker (2003).

The chemical analysis of epidote, carbonate, biotite and chlorite was made with the Electron Probe Micro Analyzer (EPMA), Cameca SXFive model, directly into the thin sections coated with carbon at the Laboratory of Electronic Microprobe in the Center of Studies in Petrology and Geochemistry (CPGq). The energy conditions of the analysis by EPMA were of 15 kV and 15 nA, with a beam of 5 μm diameter, without considering analysis of chlorites whose sum of Ca, Na and K exceeded 0.5 wt.% oxides (Jiang *et al.* 1994, De Caritat *et al.* 1993, Bourdelle *et al.* 2013). Samples of chlorite were obtained by manual separation and selection with binocular stereo microscope for analysis through Mössbauer Spectroscopy (MS) in the Laboratory of the Institute of Physics at the Federal University of Rio Grande do Sul (UFRGS) using transmission with constant acceleration and cobalt 57 source in rhodium matrix. The isomeric displacement was made considering the metallic iron, with adjustment of the minimum square curve admitting Lorentzianes absorption lines.

The modelling of chlorite formation temperatures was made based on chemical data obtained with the electronic microprobe, correcting a Fe^{2+}/Fe^{3+} ratio by MS as stated in the methodology proposed by Inoue *et al.* (2009) and Inoue *et al.* (2010). The analysis and classification of the chlorite polytypes were made by diffractometry X-ray with Siemens equipment, model Bruker-AXS D5000, installed at the CPGq, using the CuKα radiation with energy conditions of 40 kV and 25 mA. The isotopic analysis of $δ^{13}C_{VPDB}$ e $δ^{18}O_{VSMOW}$ of calcites collected by manual selection under binocular magnifying glass was conducted at the Laboratory of Isotopic Geology of CPGq, with the IRMS Delta V Advantage — Gas Bench equipment using the standards NBS 18, IAEA-CO8, IAEA-CO1 and REI.

RESULTS

Field and petrographic observations

In the studied region of the ISZ, the SMCGC orthogneisses present fault planes that contain lineation of NW direction, which delimit a subvertical and transcurrent shear zone. In the fault system planes, reactivations of the gneissic banding (N68E/84NW) and slickensides occur, which register a sinistral movement of the ISZ that indicate late movement in shallow condition of rigid blocks. Intense chloritization is described on these planes, which is associated with carbonates and hematite, indicating pervasive fluid percolation parallel to banding (NE) (Figs. 2A and 2B) with calcites that caused brecciation in the rock portions (Figs. 2C and 2D).

The petrographic analysis reveals that the banding is set by millimetric layers enriched in phyllosilicates, interleaved with quartz-feldspathic bands. The essential mineralogy of the studied orthogneisses consists of quartz, plagioclase, biotite, muscovite, chlorite, epidote, albite, and calcite (Tab. 1), in addition to zircon and apatite as accessory minerals. The orthogneisses show a fine-grained granoblastic texture of plagioclase and quartz. Along with the lepidoblastic texture of the phyllosilicates (biotite and muscovite), the quartz is found elongated in the banding direction, generating a metamorphic texture that is mylonitic recrystallization (Fig. 3A). The quartz is shown intensely recrystallized in two different generations, marked by the difference in the average size of the grains. Locally, the plagioclase is altered to white mica in thin lamellae (Fig. 3B). In the more chloritized samples, sericitization, albitization and epidotization of the plagioclases happens (Figs. 3C and 3D), and the epidotes do not show zonation. The chlorites occur as transformations of the metamorphic biotites. The intensity of chloritization substituting the metamorphic biotites is variable, reaching integral levels as observed in sample IB 2A (Fig. 3E).

Other hydrothermal and less expressive minerals result from the alteration. In the cleavage of these substitute chlorites, rutiles of very fine texture (Fig. 3E) appear or as needles inside the chlorites. Titanites are observed only in intensely chloritized samples, showing anhedral texture. Barites are found in rare veins with calcites. The opaques are rare and form aggregates, sometimes cubic, elongated according to the direction of banding, interpreted as pyrites and chalcopyrites on reflected light analysis; opaques with thinner texture were interpreted as ilmenites under the reflected light.

Locally, millimetric cataclastic zones were identified parallel to banding with grain fragmentation and presence of chlorite and hematite, setting the banding reworking. Carbonate veins with albite cut the banding transversally and rarely exist concomitant to chlorite, representing predominately final stages of the event of hydrothermal alteration. Individual grains and aggregates of hydrothermal quartz (Fig. 3F) and veins parallel to the banding characterized by elevated concentration of fluid inclusions are also associated with each other. In the hydrothermal alteration, the minerals that occur in paragenesis with chlorite are epidote, white mica, carbonate, titanite, rutile and ilmenite, pyrite and chalcopyrite, barite and quartz, characteristics of a propylitic alteration, typically of greenschist facies of low pressure and low to intermediate pressure (Winter 2014).

Chemical analysis of hydrothermal minerals

Epidotes, chlorites, and calcites are the most common solid solutions of hydrothermal parageneses associated with the ISZ and, due to its importance for understanding the alteration process, they were analysed in EPMA aiming at determination of their chemical composition.

Gerhard & Liebscher (2004) established a solid solution for the epidotes formed by the components clinozoisite (Czo), epidote (Ep), and tawmawite (Taw). The epidotes from the samples of the study region hold a composition (Tab. 2), in which the epidote (Ep) molecule is predominant with variation of this component of about 58 to 93% (center of grains) and 61 to 89% (edge of grains).

The carbonates analysed in the samples by EPMA (Tab. 2) are composed of 95.61 to 98.48% of $CaCO_3$, and they are classified as calcites.

The chlorite, main mineral phase of the propylitic alteration, is petrographically a substitution product of metamorphic biotite present on the orthogneiss. The analysis of the biotites that were altered to chlorite (Tab. 2) show a regular composition (Deer *et al*. 1962), with a variation of Fe/(Fe + Mg) between 0.442 and 0.489 and a participation of Al^{IV} (a.p.f.) of 2.347 to 3.194. The chlorites (Tab. 2) have a ferromagnesian composition, and the analysis that met the parameters of low Ca, Na, and K content was selected
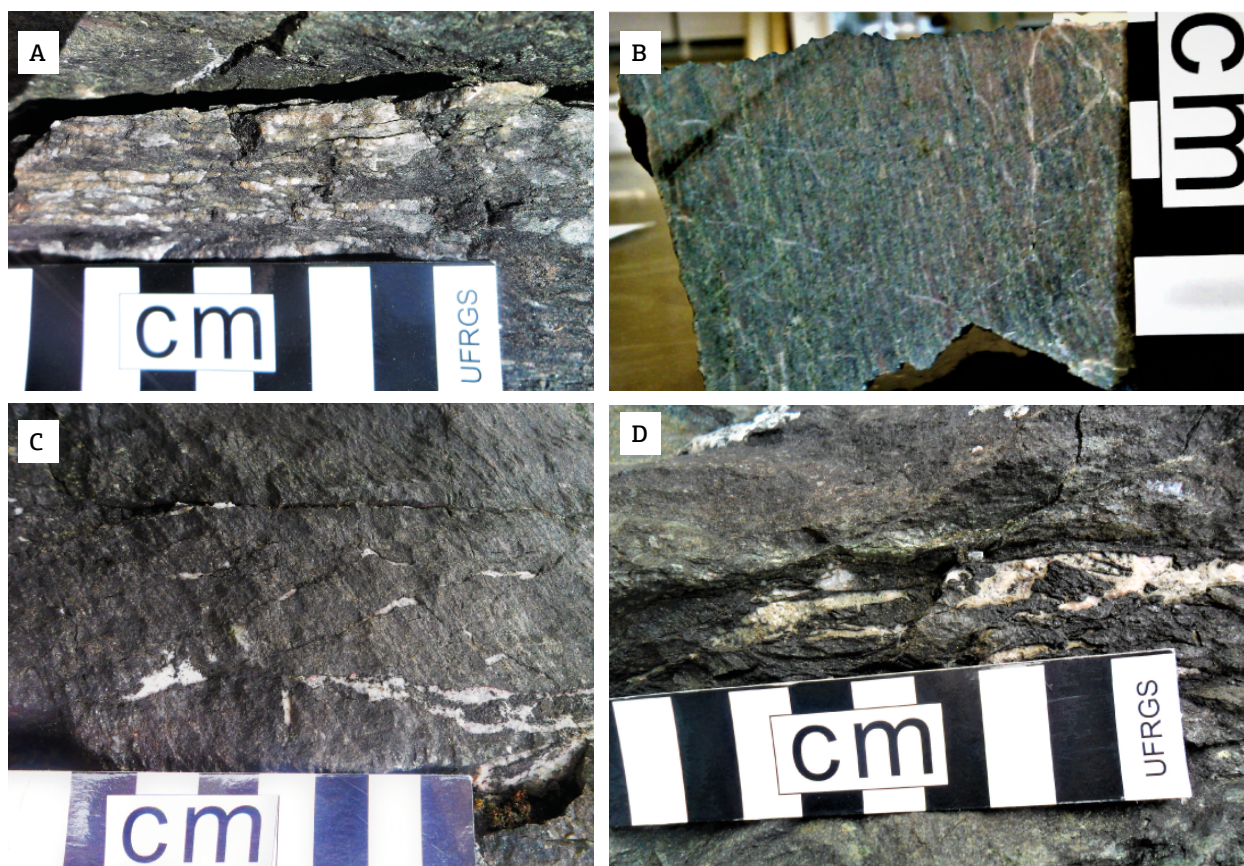

Figure 2. Macroscopic pictures of the rocks and their field relations. (A) Orthogneiss (sample IB 2A) intensely chloritized. (B) Deeply chloritized orthogneiss (sample IB 01) cut by millimetric fractures filled with carbonates. (C) Fractures and veins filled by carbonates. (D) Carbonate breccia in contact with chloritized orthogneiss.

according to Jiang *et al.* (1994), De Caritat *et al.* (1993) and Bourdelle *et al.* (2013). The Fe^{2+}/Fe^{3+} ratio of the chlorites analysed through the MS indicate an average proportion of 80.5% of Fe^{2+} and 19.5% of Fe^{3+} (Tab. 3). It has been classified as Fe-clinochlore according to Moazzen (2004) and Yavuz *et al.* (2015), as its average chemical formula obtained based on 28 equivalent oxygen, ignoring the H_2O (where $\square$ = vacancies) would be: $Mg_{5.31} Fe^{2+}_{3.25} Al^{VI}_{2.18} Fe^{3+}_{0.79} Mn_{0.04} Ti_{0.01} \square_{0.43} (Si_{5.85} Al^{IV}_{2.15}) OH_{16}$.

Physical parameters of the event

Chlorite geothermometry and paragenetic relations

The chlorite formation temperature in the ISZ was estimated according to Inoue *et al.* (2009) and Inoue *et al.* (2010). Differently from the empirical approach (Cathelineau & Nieva 1985, Cathelineau 1988, Kranidiotis & MacLean 1987, Jowett 1991, De Caritat *et al.* 1993, and others) and of the first chemical geothermometers (Walshe 1986, Vidal *et al.* 2001), the thermodynamic model represents the natural system of ferromagnesian trioctahedral chlorite formation

Table 1. Analysis of modal composition of the orthogneisses from unaltered SMCGC (sample IB 5A) and with hydrothermal alteration (samples IB 01 and IB 2A).

| Mineralogy	IB 01 (%)	IB 2A (%)	IB 5A (%)
Quartz generation 1 (Met.*)	36.56	18.92	22.82
Quartz generation 2 (Met.)	–	–	22.09
Plagioclase (Met.)	–	1.08	11.63
Plagioclase sericitized	15.51	19.69	1.74
Biotite (Met.)	–	–	29.22
Muscovite (Met.)	0.77	0.92	11.48
Quartz (Hidr.**)	–	24.00	–
Chlorite (Hidr.)	24.88	22.00	0.43
Epidote (Hidr.)	9.68	2.92	–
Sericite (Hidr.)	–	2.31	–
White Mica (Hidr.)	2.76	4.62	–
Albite (Hidr.)	3.38	2.15	–
Carbonate (Hidr.)	4.61	0.15	0.15
Hematite (Hidr.)	1.38	–	–
Opaque	0.46	1.23	0.44
Total	100	100	100
Total points	650	650	650

*Met: metamorphic; **Hydr.: hydrothermal.

more properly in low to intermediate temperatures and with considerable amounts of Fe^{3+} (> 14% of total Fe). The utilization of the geothermometer is recommended in systems that work with water and SiO_2, as observed in the ISZ. The calibration of the chlorite geothermometer uses a relation between temperature (1/T) and the equilibrium constant (K) of the reaction, which involves the end members of the chlorite of interest (Inoue *et al.* 2009). Applying the methodology, the temperature values found for the hydrothermal chlorites formed by the metamorphic biotite varied from 191 to 352°C (Fig. 4), with an average formation temperature converging to 274°C.

Considering the studied system, the qualitative verification of the temperatures obtained with the chlorite geothermometer was made by observing certain properties of the associated hydrothermal phases, through the determination of chlorite polytype, texture and mineral assemblage. The hydrothermal chlorites of this study show a structure that classified them inside the polytype II*b* (Fig. 5A), whose environment of formation implicates in temperatures above 200°C (Walker 1993). In some of the associated calcite grains, twins were identified with an irregular pattern of thickness (Fig. 5B), which indicate an early crystallization in temperatures above 250°C (Ferrill *et al.* 2004). The paragenesis of the hydrothermal event of this study (Fe-clinochlore, epidote, albite, white mica, calcite, titanite, rutile and ilmenite, barite, pyrite and chalcopyrite, quartz) indicates a propylitic alteration of the orthogneiss in low pressure and low to intermediate temperature conditions, in a Na-Mg-Fe-Ca system depleted in K (Kühn 2004). The paragenesis (Fig. 5C) indicates low-pressure formation conditions in the order of < 2,000 bar, range of temperature between 100 and 300°C, and fluids with neutral to slightly alkaline pH (Pirajno 2009, Winter 2014). At the epithermal system, the conditions of formation of rutile, quartz and epidote enter the temperatures given by the chlorite in the ISZ. The pyrite and calcite formation is in accordance with the range of temperature obtained. However, its occurrence may extent to approximately 100°C, in which the calcite veins of lower temperature would represent the final stages of the event.

Fluid inclusions

The FIs analysis was carried out in quartz samples belonging to the gneiss, with granoblastic texture, and from veins associated with the gneiss fracture parallel orientation to the banding, with domains of the vein having granoblastic texture. The quartz vein includes chlorite aggregates, suggesting a late fluid when compared to the chloritization process. The FIs are found in secondary trails of the two-phase and aqueous type, and one-phase clear and aqueous
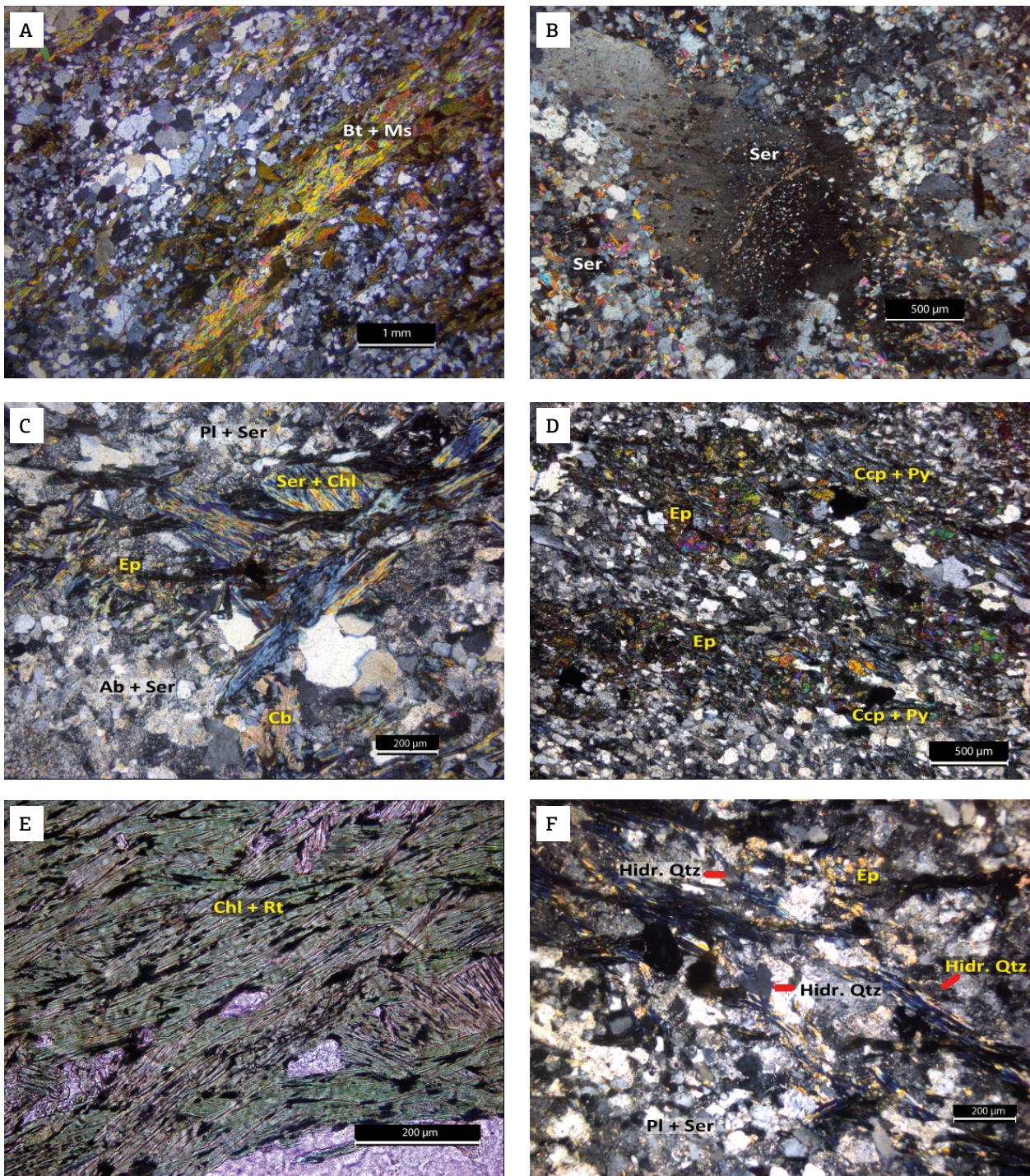
Ab: albite; Bt: biotite; Cb: carbonate; Ccp: chalcopyrite; Chl: chlorite; Ep: epidote; Hydr. Qtz: hydrothemal quartz; Ms: muscovite; Pl: plagioclase; Py: pyrite; Rt: rutile; Ser: sericite.

Figure 3. Petrographic aspects under polarized light on orthogneissic samples of unaltered SMCGC and with hydrothermal alteration collected in the study area. (A) Sample IB 5A: Primary biotites and muscovites with lepidoblastic texture. (B) Sample IB 5D: Sericite with fine texture generated by the alteration of primary plagioclase. (C) Samples IB 2A: Sericitization, albitization and epidotization of primary plagioclase and sericite generated through biotite alteration. (D) Sample IB 01: Intense epidotization, pyrite and chalcopyrite. (E) Sample IB 2A: Intense chloritization and formation of chlorites from the substitution of biotites; rutiles included in chlorites as the product of reaction of decomposition of biotite. (F) Sample IB 2A: Presence of hydrothermal quartz.

Table 2. Summary of chemical analysis (wt.%) through EPMA of the main minerals involved on the alteration (epidote, carbonate, biotite and hydrothermal chlorites). The standard analysis represents a typical analysis of the minerals in the sample. For the chlorites, the values with contamination > 0.5%wt. were discarded and not included.

Sample	EPIDOTE				CARBONATE				BIOTITE		CHLORITE			
	IB 01				IB 01		IB 5C		IB 5A		IB 01	IB 2A	IB 32A	
Analysis	Stan. Point 21-Centre	Stan. Point 21-Edge	Av. Centre (n = 40)	Av. Edge (n = 36)	Stan. Point 18 - Centre	Av. (n = 85)	Stan. Point 1 - Centre	Av. (n = 45)	Stan. Point 74-Centre	Av. (n = 85)	Stan. Point 01-Centre	Stan. Point 17-Centre	Stan. Point 78 – Centre	Total Average (n = 178)
SiO_2	37.57	37.39	37.46	37.46	–	–	–	–	36.02	35.56	27.65	28.09	28.75	27.98
Al_2O_3	23.37	23.05	23.86	23.86	–	–	–	–	17.03	17.17	17.31	17.68	17.75	17.59
Fe_2O_3	13.64	13.6	12.92	12.93	–	–	–	–	–	–	–	–	–	–
FeO	–	–	–	–	0.05	0.04	0.2	0.22	18.14	18.43	23.65	23.51	21.39	23.36
MgO	0.01	nd	0.01	0.01	nd	0.01	0.07	0.12	11.36	11.58	16.08	17.2	18.53	16.75
MnO	0.04	0.08	0.09	0.09	0.08	0.08	0.69	0.78	0.12	0.15	0.27	0.27	0.21	0.25
TiO_2	0.04	0.02	0.05	0.05	–	–	–	–	2.25	2.14	0.06	0.03	0.12	0.07
Na_2O	nd	0.03	nd	0.01	–	–	–	–	0.12	0.13	0.03	0.01	0.01	0.01
K_2O	0.01	0.01	0.01	0.01	–	–	–	–	9.61	8.94	nd	0.02	nd	0.05
CaO	23.17	23.28	23.25	23.26	55.88	55.99	54.25	54.29	nd	0.01	0.08	0.03	0.01	0.06
Cr_2O_3	–	–	–	–	–	–	–	–	0.1	0.1	nd	0.06	0.14	0.04
SrO	–	–	–	–	0.02	0.04	0.4	0.41	–	–	–	–	–	–
BaO	–	–	–	–	nd	0.02	0.02	0.01	–	–	–	–	–	–
Y_2O_3	nd	nd	0.01	0.01	–	–	–	–	–	–	–	–	–	–
La_2O_3	0.06	0.03	0.02	0.02	–	–	–	–	–	–	–	–	–	–
Ce_2O_3	0.01	0.03	0.04	0.04	–	–	–	–	–	–	–	–	–	–
Nd_2O_3	nd	0.01	0.01	0.01	–	–	–	–	–	–	–	–	–	–
Total	97.91	97.52	97.74	97.76	–	–	–	–	94.75	94.19	85.12	86.9	87.06	86.16
CO_2 (c)	–	–	–	–	43.96	43.83	44.37	44.18	–	–	–	–	–	–
H_2O (c)	1.88	1.87	1.88	1.88	–	–	–	–	3.92	3.90	11.53	11.41	11.57	11.51
Total (c)	**99.79**	**99.39**	**99.62**	**99.64**	**100**	**100**	**100**	**100**	**98.67**	**98.09**	**96.65**	**98.31**	**98.63**	**97.69**
Czo (%)	18.89%	17.42%	22.50%	22.56%										
Ep (%)	81.11%	82.58%	77.50%	77.44%										
Taw (%)	0%	0%	0%	0%										

Av.: average; Czo: clinozoizite; Ep: epidote; Stan.: standard; Taw: tawnawite; (c): calculated using Cameca SXFive analysis routine; (nd): not detected; (-): not analysed.

Table 3. Data of hydrothermal chlorite analysis by Mössbauer Spectroscopy (MS).

Sample	EQ 1 (mm/s)	IS 1* (mm/s)	Wid Lin 1 (mm/s)	Area 1	EQ 2 (mm/s)	IS 2* (mm/s)	Wid Lin 2 (mm/s)	Area 2	EQ 3 (mm/s)	IS 3* (mm/s)	Wid Lin 2 (mm/s)	Area 3
IB 01	2.62	1.13	0.36	0.79	–	–	–	–	0.98	0.40	0.84	0.21
IB 2A	2.62	1.13	0.33	0.82	0.68	0.25	0.49	0.14	0.97	0.52	0.31	0.04

*Relative to metallic iron. EQ: quadrupolar interaction (mm/s); IS: isomeric displacement in relation to metallic Fe (mm/s); Wid Lin: width of line (lorentziane) (mm/s); Area: proportion of each sub-spectra: area 1 represents the Fe^{+2} and areas 2 and 3, the Fe^{3+}.

type (Fig. 6A), and one-phase containing accidental solids of carbonates and other non-identified minerals.

Although the inclusions are numerous in quartz veins or in the gneiss (Fig. 6B), only some FIs had compatible dimensions for the technique application by fluid inclusion microthermometry. Along the limits of the quartz grains, we observed dark FIs due to the leakage of the fluids imprisoned during the secondary quartz growth. FIs with indicative textures of necking-down were not considered in the analysis when possible.

The measurements were made in two-phase and aqueous FIs associated with secondary trails, with temperatures of the end fusion of ice (Tf) obtained in the presence of the gas phase (Tab. 4). The FIs system is NaCl-H_2O, with gas volume related to the total cavity of inclusion of 10 to 28% and dimensions between 5 and 27.5 μm. Metastable inclusions also occur, indicated by the disappearance and non-returning of the bubbles even after the fusion of ice, as it occurred with the IFs on quartz from the interior of the gneiss. The metastability is detected on the experiments due to the difficulty of creating a core of bubble gas during the heating, causing errors in the measurements. The origin of the metastability condition is diverse and can be linked to factors like irregularity in the FIs' shape, position of the inclusion inside the crystal, superficial tensions inside the inclusion, negative pressure and nucleation difficulties of the FI chemical system (Roedder 1971, 1984).

The analysis of FIs established only one family of inclusions, and the obtained results show that the Tf occurred in the interval between -0.8 and -2.1°C, with an average of -1.4°C. Homogenization temperatures (Th) occurred in the interval between 110.8 and 238.9°C, with an average of 175.16°C (excluding the FIs that presented metastability in both vein and gneiss). The salinity varies from 1.1 to 4.3%, with an average of 2.45 wt.% NaCl eq., not having
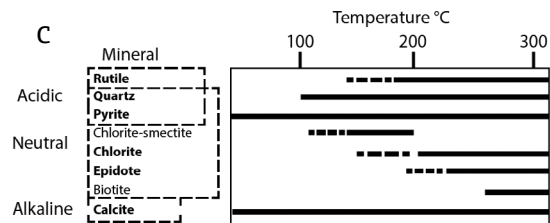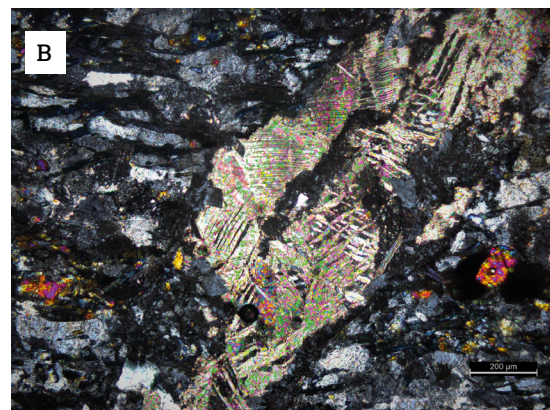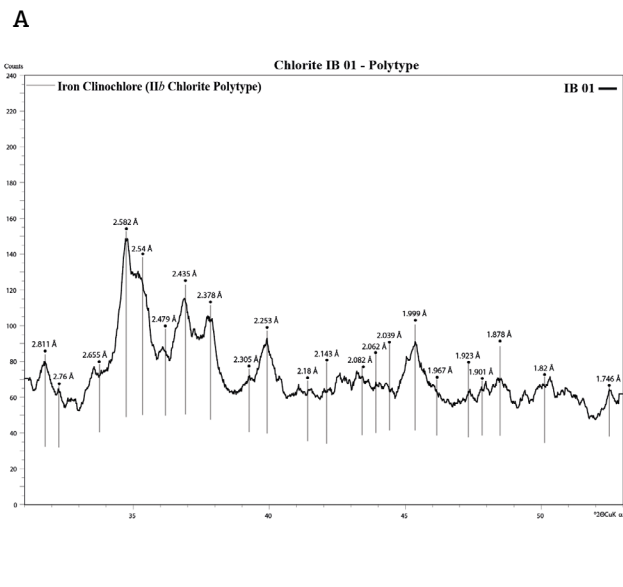

Figure 4. Temperature values at ISZ obtained in this study with the chlorite geothermometer using the chemical approach (thermodynamic) of Inoue *et al.* (2009). The analysis with sum in wt.% of the oxides of Ca, Na and K above 0.5% were not used.

Figure 5. (A) Analysis of the polytype II*b* of the ISZ hydrothermal chlorites (samples IB 01) (X-ray diffraction obtained through the interval from 31 to 53° 2δ). (B) Calcite texture with twinning elements of irregular thickness identified in the ISZ (sample IB 01, optical microscope, polarized light, scale 200 mμ). (C) Mineral phases associated with the alteration process in the ISZ, regarding the respective intervals of temperature and pH observed in epithermal events (modified from Pirajno 2009).

a modal value between the most recurrent values of temperature (160 to 170°C). The NaCl-H$_2$O composition creates an aqueous electrolytic and binary system important to modelling fluids of several environments (Bodnar & Vityk 1994), including shallow systems (epithermal).

The volumetric properties of the fluid phase (density and specific volume) are projected in a P-T evolution using isochores (Knight & Bodnar 1989). From the salinity of the FI with lower Th and most reliable measure (1.396 wt.% NaCl; 163.4°C), it is possible, through the routine *AqSo1e™* based on Bodnar (1993), to determine the density of the NaCl-H$_2$O system, in which, in this case, it was estimated in 1.01566 g/cm^3 to 25°C. In the same way, to the FI with the most reliable Th (196°C; 2.24053 wt.% NaCl), the calculated density of the NaCl-H$_2$O system was 1.02198 g/cm^3 at 25°C.

Stable isotopes

On the carbonate samples of the ISZ, we measured the variation of the stable $\delta^{13}C_{VPDB}$ and $\delta^{18}O_{V\text{-}SMOW}$ isotopes with the aim to obtain information about the hydrothermal fluids' origin. The results show that the carbonates related to the ISZ and to the event of chloritization (Tab. 5) vary from -5.55 to -7.43 $\delta^{13}C_{VPDB}$ and from 8.29 to 16.81 $\delta^{18}O_{V\text{-}SMOW}$. The occurrence range of carbon isotopes of carbonates of the ISZ associated with the chloritization marks behavior of mantellic origin (Fig. 7A). On the other hand, the oxygen isotopes show a wider compositional range, encompassing possible source of juvenile, metamorphic, mantellic and meteoric water (Fig. 7B).

DISCUSSION

In the hydrothermal alteration parageneses, minerals can be identified, which form solid solutions with compositional variations susceptible to modifications that balance the minerals according to the environment thermodynamic and geochemical signatures. The capacity of the minerals that form solid solutions to adapting to variations, especially in temperature, pressure and/or presence of CO$_2$, produces compositional variations used for defining the stability fields
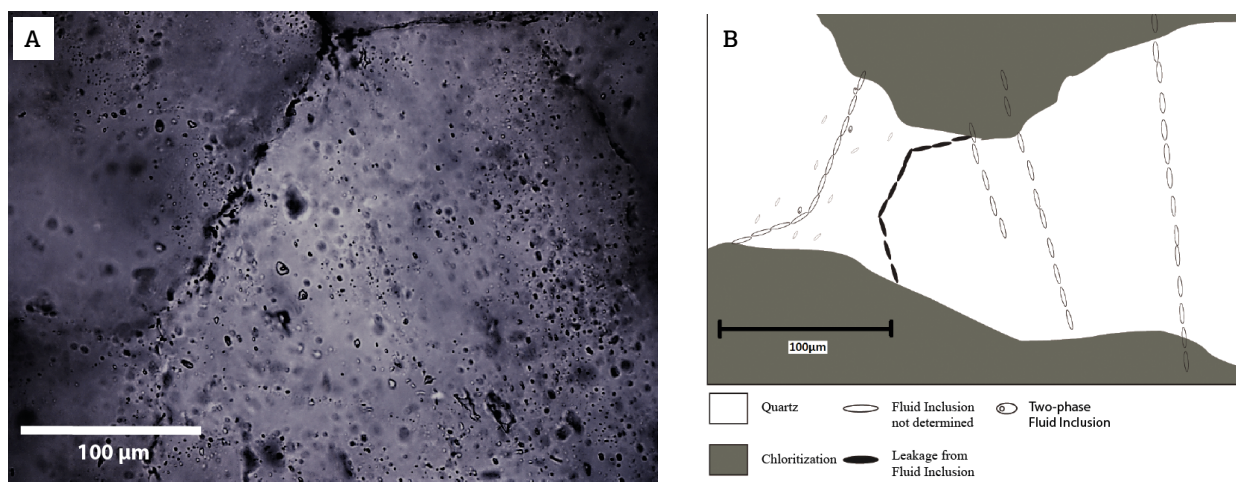

Figure 6. Mode of occurrence of fluid inclusions (FIs) in the sample IB 2A associated with the quartz vein or inside the quartz of the gneissic banding in the ISZ. (A) Quartz vein containing secondary trails of two-phase and one-phase clear and aqueous FIs and dark inclusions attributed to the empty at the edge of the grains (optical microscope, polarized light with plane-polarized light). (B) Schematic representation of quartz in gneissic banding containing two-phase FIs of small dimensions, which made trustworthy measuring with the adopted methodology impossible (measures of metastable type).

Table 4. Parameters obtained through measurements of the FIs (sample IB 2A) of ISZ by the secondary FIs in quartz from hydrothermal vein.

Geological context	Ibaré Shear Zone – Vein of hydrothermal quartz					
System FI-NaCl-H$_2$O	Tf °C	Th °C	V$_{gas}$ (%)	Size (µm)	Salinity (wt.% NaCl eq.)	d (g/cm³)
	-0.8 to -2.1	110.8 to 238.9	10 to 28	5 to 27.5	1.1 to 4.3	1.01566 to 1.02198

d: density; Tf: temperature of fusion of ice; Th: temperature of homogenization; V: volume.
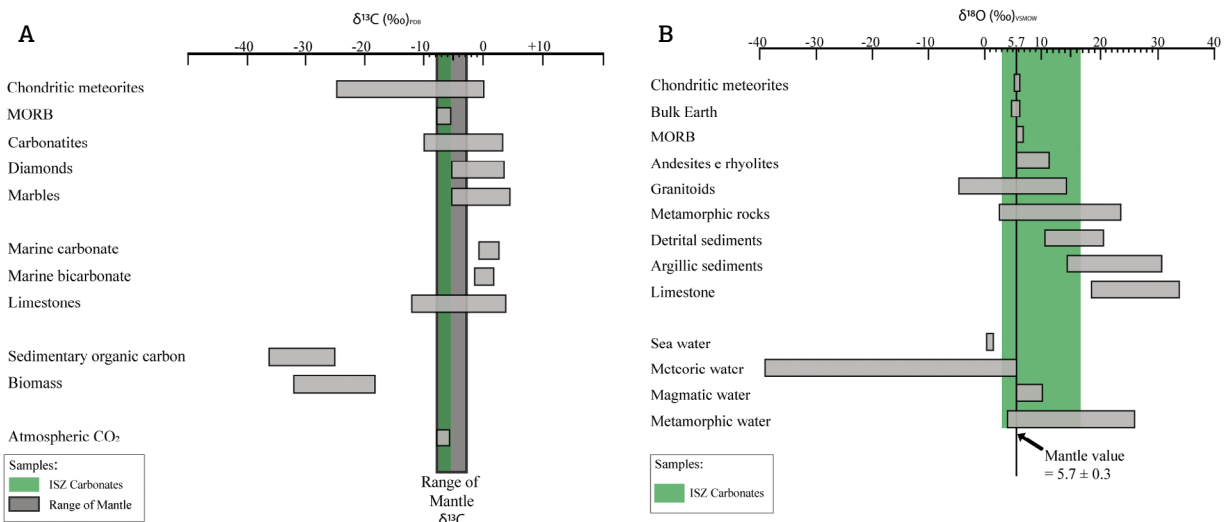
of the minerals (Beane 1994). The comprehension of the physical-chemical aspects about the alteration minerals is important to understand the event that generated the minerals, as well as its metallogenetic potentiality. The equation of the system variables, such as P-T and fluid composition, is more efficient when the complexity of the system is accounted, especially with pieces of information obtained from the minerals that form the alteration paragenesis.

The modal analysis and chemical composition of the orthogneiss studied reflect an original dioritic/granodioritic assemblage (Laux & Bongiolo 2011, Philipp *et al.* 2017, Laux 2017) by the mineralogy, with absence of potassic phases. Through the hydrothermal alteration paragenesis of the studied samples, represented by chlorite, epidote, albite and carbonate, and the stability fields of these minerals, it is possible to infer about the conditions of formation (Fig. 8A). Using the stability curves of the alteration minerals from the granitic rocks presented by Reed *et al.* (2013), it is possible to estimate the equilibrium conditions of the alteration mineralogy of the ISZ as being from a low ratio of water/rock, temperatures from approximately 250 to 300°C and from neutral to slightly acidic solutions (Fig. 8B).

Hydrothermal systems with neutral pH conditions are usually found in shallow epithermal zones (White & Hedenquist 1990), in which the heat from fluids act in superficial zones of the crust. The typically neutral composition of some epithermal systems is determined by the interaction between convective cells of meteoric fluids with the host rock and magmatic fluids, and the generation of low-temperature quartz veins is common in this condition (Heinrich 2005, Norton & Knight 1977). The fluids that rise from large depths are balanced with their host rocks and are, therefore, reduced, with a pH near the neutral level. This reaction usually sets the NaCl as one of the main species that compound the system fluids (White & Hedenquist 1995), as verified on the fluid inclusions on the ISZ quartz. This neutral pH is compatible with the propylitic alteration

Table 5. Isotope ratios of δ^{13} C and δ^{18} O from carbonates associated with fault planes of the ISZ (chloritization).

No. Lab.	Field name	Carbonates	
		δ^{13} C$_{VPDB}$‰	δ^{18} O$_{V\text{-}SMOW}$‰
1	CARB 1	-6.46	16.81
2	CARB 2B	-5.55	9.40
3	CARB 2C	-7.07	5.75
4	CAR 1	-6.55	7.05
5	CAR 2	-5.87	14.44
6	CAR 3	-6.14	9.18
7	CAR 5	-6.52	3.02
8	CAR 6	-6.57	6.33
9	CAR 7	-6.16	11.64
10	MIL 01	-7.43	8.94
11	GNA 03	-6.72	8.29

Figure 7. Values of δ^{13} C$_{VPDB}$ e δ^{18} O$_{VSMOW}$ from several environments and terrestrial processes (modified from Rollinson 1993). (A) The range of carbon isotopes occurrence for the ISZ carbonates is distinguished by a juvenile origin of the alteration solutions. (B) The range of oxygen isotopes occurrence presents a broad variation, encompassing possible sources of juvenile, metamorphic, mantellic, and meteoric fluids. The isotopic composition of oxygen in carbonate is a function of its provenance, but modified (fractions) by several mechanisms — one of the parameters is the deposition temperature.

identified, since the acidic solutions favour the formation of argillic alteration (Shikazono 2003).

The hydrothermal alteration characteristics are influenced by variables such as fluid chemical composition, temperature, fluid volume and water/rock interaction and the host rock type (Shikazono 2003, Harlov & Austrheim 2013). The chloritization verified in these orthogneisses, which is a subdivision of a propylitic alteration, usually substitutes the phyllic alteration in dioritic rocks, reflecting a higher content of mafic minerals in those rocks, due to the control of the initial host rock composition under the alteration mineralogy (Beane 1994). The low abundance of sulfides in the hydrothermal paragenesis can be linked to the small amount of primary minerals composed by iron or of fluid with low content of sulphur species and, therefore, with low capacity of gold solubilization, which would reflect a sub economic prospect of the possible deposit (Yamaguti & Villas 2003). Hydrothermal environments with low salinity and low content of sulphides, as the one observed in the ISZ, are usually associated with fluids of neutral pH and low temperature, as a result of the mixture of juvenile fluid with meteoric water in shallow regions of the crust, far from the related intrusions (White & Hedenquist 1995, Biondi 2003).

Propylitic alterations are typical of the interaction with meteoric fluids, because they occur mainly in zones with entrance of meteoric fluids in hydrothermal systems (Pirajno 2009), favoured in the ISZ by faulting. This mixture of fluids

promoted Na-Mg-Ca metasomatism, leaching most part of K and favouring the generation of albites in relation to the K-feldspars (Kühn 2004), which are accentuated by the dioritic/granodioritic character of the host orthogneisses. The albite formation is characteristic of the propylitic alteration and occurs by heating of the host rocks and by the interaction with the descendent flux of fluids in the recharged zone of the hydrothermal system (Shikazono 2003).

The K leaching may be observed in the ISZ through the lack of hydrothermal minerals that bring K to their structure, which allows the interpretation that K comes from the alteration of muscovites, biotite and plagioclase contained in the orthogneiss and that K was leached, being only a small portion kept on the structure of sericites. Regarding the epidote, the main compositional change is monitored by the substitution of Fe^{3+} and Al ions in its octahedral site (Gerhard & Liebscher 2004). The Fe^{3+}/Al ratio on epidote is dependent on the variation of temperature, pressure, f_{O_2}, conditions of oxi-reduction and chemical composition of the system. Epidotes formed in low temperature and pressure conditions tend to be enriched in Fe^{3+} in relation to Al, such as the epidotes formed only by feldspar albitization that tend to be more aluminous (Grapes & Hoskin 2004, Phillips *et al.* 2010). In hydrothermal systems with oxidizing to reducing conditions, the epidote collapse temperature is smaller, which decreases the Fe^{3+}/Al ratio and becomes more aluminous (Holdaway 1972). Epidotes in hydrothermal systems with high P_{CO_2} usually present
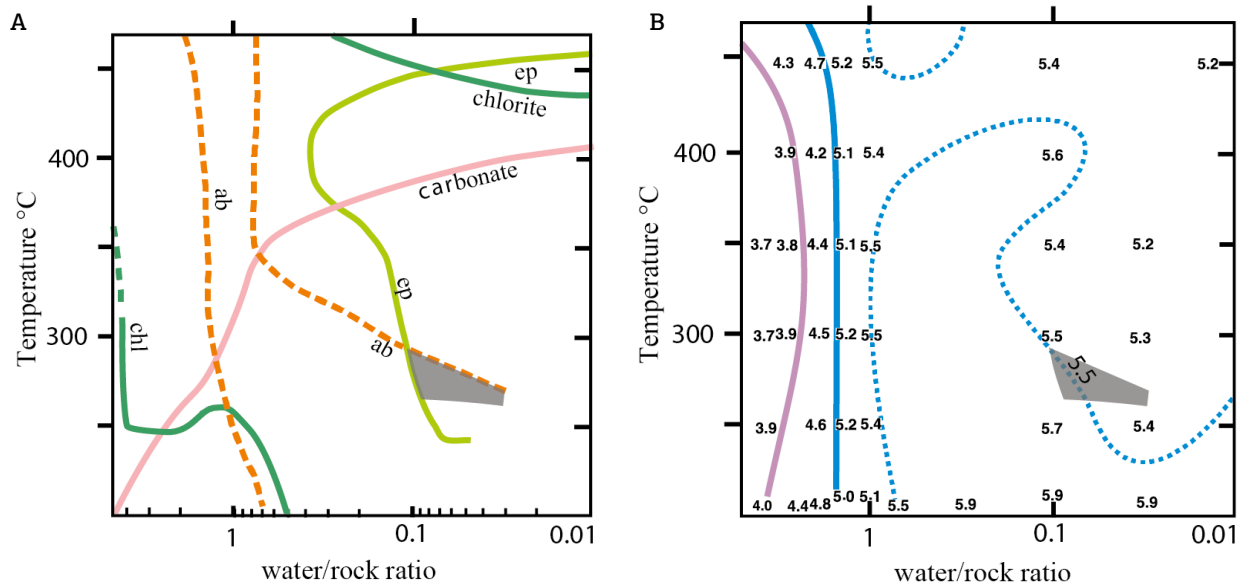
ab: albite; chl: chlorite; ep: epidote.

Figure 8. Determination of parameters of solutions and temperature at the ISZ from stability diagrams of the alteration minerals presented by Reed *et al.* (2013). The marked areas on the diagrams are according to the initial phases of the hydrothermal alteration system in the ISZ. (A) Stability curves of the minerals as a function of the ratio water/rock and temperature (°C). (B) From the position of the ISZ observed in the stability diagram of Fig. 7A, the probable pH condition of the alteration solutions can be determined at the ISZ.

zonation with a core enriched in Fe^{3+} and edged enriched Al, suggesting isothermal conditions. The P_{CO_2} significantly controls the epidote composition (Freedman *et al.* 2009). The limit between the two generations of epidotes can be sharp (zonations) or gradual, depending on the variation history of rock temperature and diffusivity of Fe^{3+} and Al. A variation between 10-20% of Fe^{3+}/Al (Grapes & Hoskin 2004) is common. Although there is a compositional variation of the hydrothermal epidotes of the ISZ, there is always a predominance of ferric composition, indicating lower temperatures compatible with the hydrothermal system. Changes on the P_{CO_2} conditions, during the carbonatation phases, and shift of f_{O_2} and oxi-reduction conditions for a more oxidizing environment during the entrance of meteoric fluids can be the controller of this relatively large composition field of epidotes.

The average temperature of 274°C obtained for the formation of chlorites is according to the propylitic model, far from the source of juvenile fluids and with the possibility of interaction with meteoric fluids of the descending recharge zone of the hydrothermal system (Norton & Knight 1977, White & Hedenquist 1995, Shikazono 2003, Pirajno 2009). The relations between the temperatures found on the chlorite geothermometry with the ones found in FIs (Fig. 9) allow the affirmation that the chloritization was developed from higher to moderate temperatures of the initial stage of the propylitic hydrothermal system, under strong influence of juvenile fluids. This model is corroborated by the behavior of the carbon stable isotopes. The lowest temperatures found

by the FIs with an average of 175.16°C evidenced a late stage of the hydrothermal system, under wider influence of meteoric fluids due to the system evolution. This interpretation is confirmed by the results of the homogenization temperature behavior and salinity of the FIs, which point to an epithermal system (Fig. 10A) with fluid mixture (Fig. 10B). In addition, the results obtained stable isotopes of oxygen of the carbonates that indicate a mixture of sources and fluids, including the contribution of meteoric water.

The temperatures obtained by the chlorite geothermometer to the ISZ are consistent with qualitative indications obtained by the verification of the chlorite II*b* polytype (equilibrium structures with temperatures above 200°C). In the same way, the calcites show that its crystallization extended since the beginning of the event in higher/moderate temperatures and is compatible with the one from chlorite, represented by the textures identified with irregular thickness of the elements of twins, indicative of temperatures above 250°C (Ferrill *et al.* 2004). At the late stages of the event, with lower temperatures and probably with mixed sources of oxygen, the calcite veins were crystallized predominantly perpendicular to the textures of chloritization along banding. The hydraulic fracturing observed on the carbonate veins indicates low load pressure of the system, on a shallow depth situation, in which the fluid pressure is higher than the lithostatic one.

Starting from the values of salinity and density of the FIs that have not presented metastability or necking, we
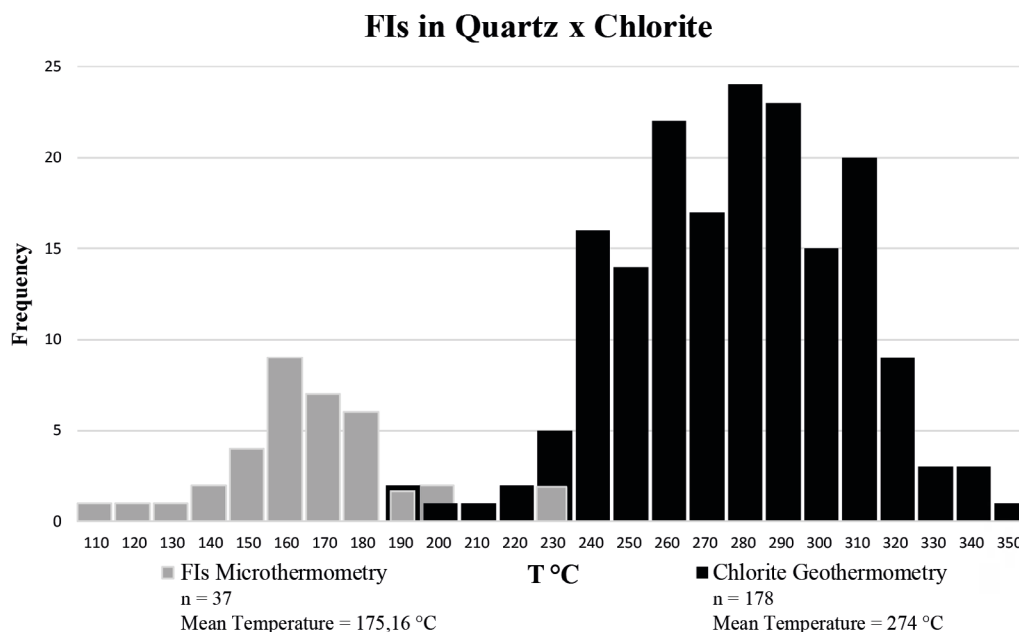

FIs in Quartz x Chlorite

Figure 9. Frequency histogram and Th of the fluid inclusions (FIs), and frequency histogram and T °C of the chlorite geothermometry. A higher temperature acting in the formation of the chloritization phases and a lower temperature on the later stages of the chloritization, dominated by meteoric fluids, are seen.

used the software ISOC™ for the definition of isochores of higher and lower Th according to Knight & Bodnar (1989) and Bodnar & Vityk (1994). At the isochore, the density of the NaCl-H_2O system stays the same under different P-T conditions and same salinity. Adjusted to this specific approach, the NaCl-H_2O fluids with salinity of
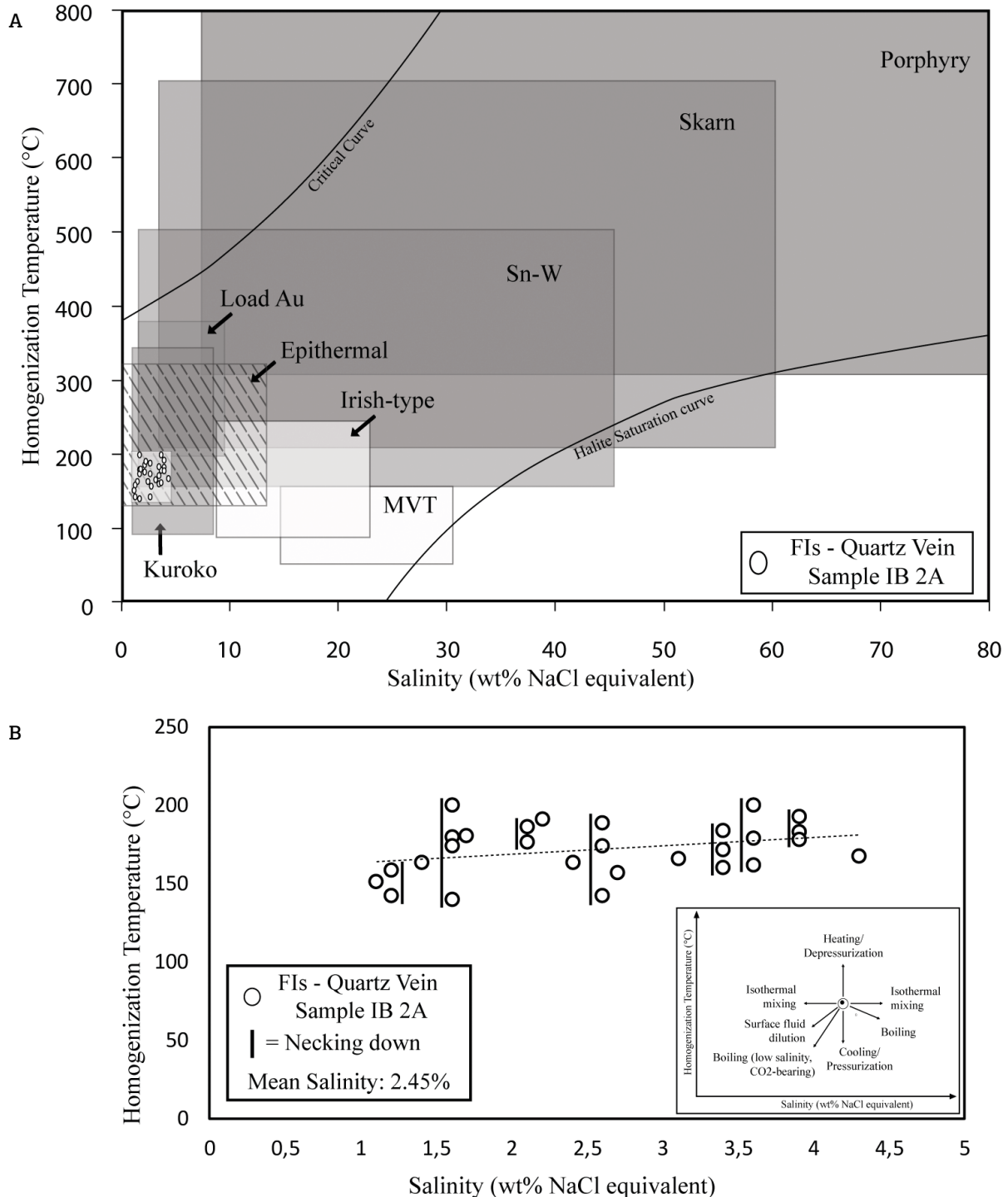

Figure 10. Results of the fluid inclusions (FIs) analysis in quartz veins on sample IB 2A of the ISZ from the diagrams of homogenization temperature (Th) and salinity (wt.% equivalent to NaCl) developed by Wilkinson (2001). (A) Regarding fields of different mineral deposits, the results obtained in the ISZ coincide with an epithermal system. (B) Only one family of inclusions is verified in a trend with strong tendency of an origin based on the isothermal mixture of fluids.

0-70 wt.% NaCl up until 6 kbars (Bodnar & Vityk 1994). This approach is applied to systems under conditions of up to 820°C, in which the error is associated with the creation of the isochore of ± 50 bars (Knight & Bodnar 1989). The interaction of isochores with the obtained temperatures with the chlorite geothermometer provides information about the possible P-T evolution of the hydrothermal event associated with the ISZ (Fig. 11). Considering the higher and lower temperatures found for the chlorite formation (352 and 191°C), we observed a variation between 3,380 and 500 bar, possibly reaching pressures near the superficial ones from the late stages of the hydrothermal alteration process. Considering the average temperature of chlorite formation of the ISZ (274°C), a pressure interval between 1,240 and 1,810 bar on the system is obtained, with an average value of 1,560 bar.

The physical parameters calculated for the hydrothermal event in the ISZ are compatible with epithermal systems that are formed in medium-low temperatures (< 300°C) and shallow depths (White & Hedenquist 1995). In this kind of system, the pressure usually is hydrostatic, commonly occurring in depths of up to 3 km (White & Hedenquist 1990), which favor the generation of veins and fragmentation by hydraulic breccias (Sillitoe 2015). Under these conditions, the dependence on structural parameters is common for permeability of fluids, as the brecciation and leaching of the components of the host rock also affect the fluid flow

(Bongiolo 2005, Henrichs 2013). Regional faults commonly have important control of epithermal systems, promoting the interaction between hot sources of deep heat with shallow systems (Panteleyev 1996). The ISZ represents a fault system that provides the establishment of a shallow hydrothermal system (Fig. 12).

As the nature of the heat source for the hydrothermal system associated with the ISZ, the obtained information with C isotopes indicated a juvenile source, while the oxygen isotopic signature values overlap the fields of the granitoids and metamorphic rocks. Thus, it indicates that the metamorphic hydrothermal fluid interacted with the juvenile source, which is in agreement with the proposed model. The results about the source are not conclusive and depend on further detailing due to the complexity observed in the ISZ. In this region, several magmatic events were found posterior to the gneisses of the SMCGC responsible for the association of plutonic and volcanic rocks, not discarding some influence of the emplacement of carbonatitic rocks (Grazia *et al.* 2011, Senhorinho 2012, Toniolo *et al.* 2013, Cerva-Alves *et al.* 2017).

CONCLUSIONS

The mineralogy identified in the hydrothermal alteration of the orthogneisses of SMCGC fits as a result of a
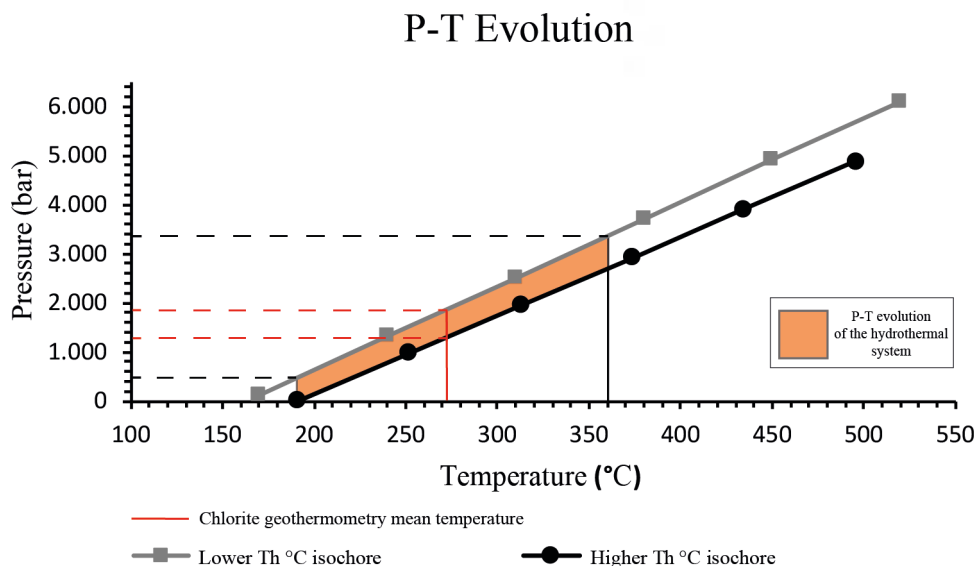

Figure 11. Evolutive behaviour of P-T on the epithermal system at ISZ obtained by data from the chlorite temperature and isochores determined under analysis of the fluid inclusions (FIs) of higher and lower reliable Th (196 and 163.4°C). The red line represents the average temperature of the chlorite geothermometer (274°C) and the orange field is the possible field of P-T evolution of the hydrothermal system.

propylitic alteration, whose mineralogy reflects a typical paragenesis of low pressure greenschist facies (< 2,000 bar). The percolation of fluids in rocks with low permeability was favoured by the reworking of the SMCGC in the study area through the ISZ, and in smaller scale by the consequent generation of hydraulic breccias and by the leaching of primary rock elements.

The hydrothermal paragenesis on the study area is composed by Fe-clinochlore, epidote, albite, white mica (sericite), calcite, titanite, rutile and ilmenite, pyrite and chalcopyrite, barite and quartz. The analysis shows that the temperature of the system varied with the hydrothermalism evolution. Initially, through the chlorite geothermometry, we obtained a higher average formation temperature of about 274°C. The detailing of the chlorite structure indicated that minerals belong to the polytype II*b*, which corroborates the obtained temperatures with the chlorite geothermometer, considering this kind of crystal lattice occurs with formation temperatures commonly over 200°C. The temperature also follows the twinning textures identified in calcites associated with chlorites, indicating temperatures over 250°C. The cooling system is set by the lowest temperatures measured through microthermometry of the fluid inclusions done in crystals of quartz, with an average of 175.16°C. The FIs also evidenced that the solutions promoting the hydrothermalism had low salinity.

The propylitic alteration is typical of zones with mixture of fluids, and the evolution of the event is compatible with hydrothermal systems in mixture zones of juvenile and meteoric fluids. Additionally, the behavior of the stable C and O isotopes indicated the presence of hot fluids of an igneous source, which cool along the withdrawal of the source and interact with the host rock and with the low-temperature meteoric fluids.

The parageneses identified in the ISZ reflect a neutral to slightly alkaline pH, marked mainly by the presence of chlorite, epidote, albite and calcite, and even apatite as accessory mineral, which is compatible with the propylitic alteration, since the acidic solutions would favour the formation of the argillic alteration. In the study region, the paragenesis is characterized by the small amount of sulphides, which are common in systems with neutral pH, developed in shallow depths and temperatures under 300°C. The neutral to slightly alkaline character of some epithermal systems is determined by the interaction of convective cells of meteoric fluids with the host rock and magmatic fluids, according to the ISZ hydrothermal model.

The pressures found to the ISZ event are of about 1,560 bar, compatible with a shallow system (epithermal). The definition of the source responsible for the high temperature fluids in the study area is complex and depends on wider detailing, given that the ISZ controls the arrangement of several magmatic bodies in the Sulriograndense Shield. The hydrothermal fluids, as indicated
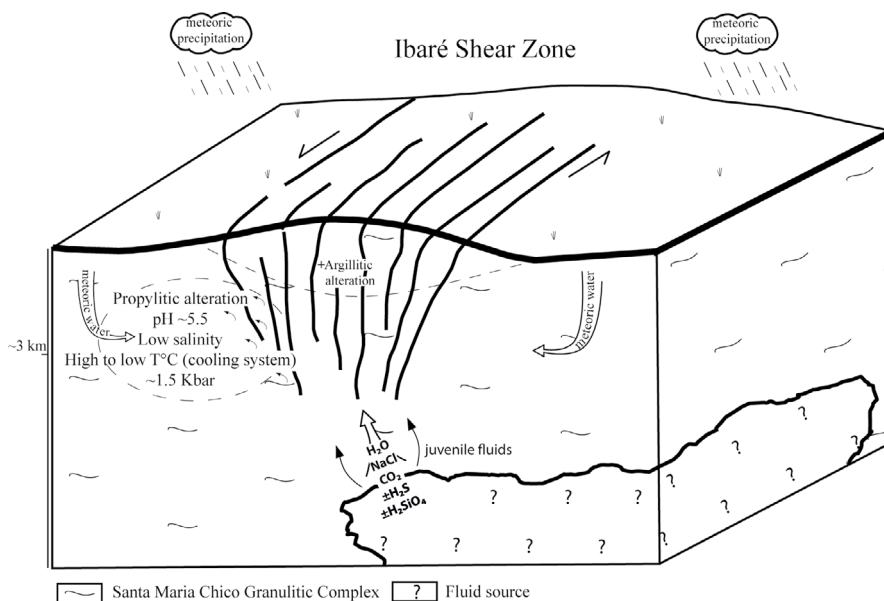

Figure 12. Schematic model idealized for the hydrothermal system that generated the chloritization in the Ibaré Shear Zone (ISZ).

by the δ^{13}C data, initially indicate a juvenile origin, while the δ^{18}O isotopes show a larger range due to the isotopic fractionation generated by the interaction of this juvenile fluid with the bulk rock and activity of the shear zone, starting to present both a juvenile and a metamorphic signature. Nevertheless, new exploration campaigns in the area should into take account the identified type and pattern of alteration and its possible association with epithermal deposit.

REFERENCES

Bakker R.J. 2003. Package FLUIDS 1. Computer programs for analysis of fluid inclusion data and for modeling bulk fluid properties. *Chemical Geology*, **194**(1-3):3-23. https://doi.org/10.1016/S0009-2541(02)00268-1

Beane R.E. 1994. A Graphic View of Hydrothermal Mineral Stability Relations. *In*: Lentz D.R. (Ed.), *Alteration and Alteration Processes associated with Ore-forming Systems*. St. John's: Geological Association of Canada, p. 1-30.

Biondi J.C. 2003. *Processos metalogenéticos e os depósitos minerais brasileiros*. São Paulo: Oficina de Textos, 528 p.

Bodnar R.J. 1993. Revised equation and table for determining the freezing point depression of H_2O-NaCl solutions. *Geochimica et Cosmochimica Acta*, **57**(3):683-684. http://dx.doi.org/10.1016/0016-7037(93)90378-A

Bodnar R.J. 2003. Introduction to aqueous-electrolyte fluid inclusions. *In*: Samson I., Anderson A., Marshall D. (Eds.). *Fluid Inclusions, Analysis and interpretation*. Vancouver, Short Course Series, v. 32, p. 81-100.

Bodnar R.J., Vityk M.O. 1994. Interpretation of microthermometric data for H_2O-NaCl fluid inclusions. *In*: De Vivo B., Frezzotti M.L. (Eds.). *Fluid Inclusions in minerals: Methods and Applications*. Blacksburg: Virginia Tech, VPI Press, p. 117-130.

Bongiolo E.M. 2005. *Depósitos Hidrotermais em Arcos Magmáticos e Alterações Associadas*. PhD Thesis, Instituto de Geociências, Universidade Federal do Rio Grande do Sul, Porto Alegre, 63 p.

Bourdelle F., Parra T., Chopin C., Beyssac O. 2013. A new chlorite geothermometer for diagenetic to low-grade metamorphic conditions. *Contributions to Mineralogy and Petrology*, **165**(4):723-735. http://dx.doi.org/10.1007/s00410-012-0832-7

Cathelineau M. 1988. Cation site occupancy in chlorites and illites as a function of temperature. *Clay Minerals*, **23**(4):471-485. http://www.minersoc.org/pages/Archive-CM/Volume_23/23-4-471.pdf

Cathelineau M., Nieva D. 1985. A chlorite solid solution geothermometer. The Los Azufrez (Mexico) geothermal system. *Mineralogy and Petrology*, **91**(3):235-244. https://doi.org/10.1007/BF00413350

Cerva-Alves T., Remus M.V.D., Dani N., Basei M.A.S. 2017. Integrated field, mineralogical and geochemical characteristics of Caçapava do Sul alvikite and beforsite intrusions: A new Ediacaran carbonatite complex in southernmost Brazil. *Ore Geology Reviews*, **88**:352-369. http://dx.doi.org/10.1016/j.oregeorev.2017.05.017

Chemale Jr. F. 2000. Evolução Geológica do Escudo Sul-Rio-Grandense. *In*: Holz M., De Ros L.F. (Eds.). *Geologia do Rio Grande do Sul*. Porto Alegre: CIGO/UFRGS, p. 13-52.

De Caritat P., Hutcheon I., Walshe J.L. 1993. Chlorite geothermometry: a review. *Clays and Clay Minerals*, **41**(2):219-239. http://dx.doi.org/10.1346/CCMN.1993.0410210

Deer W.A., Howie R.A., Zussman J. (Eds.). 1962. *Rock-Forming Minerals - 3: Sheet Silicates*. London: Longmans, 270 p.

Fernandes L.A.D., Tommasi A., Porcher C.C. 1992. Deformation patterns in the saouthern Brazilian branch of the Dom Feliciano Belt: A reappraisal. *Journal of South American Earth Sciences*, **5**(1):77-96. https://doi.org/10.1016/0895-9811(92)90061-3

Ferrill D.A., Morris A.P., Evans M.A., Burkhard M., Groshong Jr. R.H., Onasch C.M. 2004. Calcite twin morphology: a low-temperature deformation geothermometer. *Journal of Structural Geology*, **26**(8):1521-1529. http://dx.doi.org/10.1016/j.jsg.2003.11.028

Freedman A.J.E., Bird D.K., Arnórsson S., Fridriksson T., Elders W.A., Fridleifsson G.Ó. 2009. Hydrothermal Minerals Record CO_2 Partial Pressures In The Reykjanes Geothermal System, Iceland. *American Journal of Science*, **309**(9):788-833. http://dx.doi.org/10.2475/09.2009.02

Gastal M.C.G., Ferreira F.J.F. 2013. Discussão dos processos de construção do complexo granítico São Sepé, RS: feições geológicas e petrográficas. *Pesquisas em Geociências*, **40**(3):233-257. https://doi.org/10.22456/1807-9806.43440

Gerhard F., Liebscher A. 2004. Physical and Chemical Properties of the Epidote Minerals – An Introduction. *Reviews in Mineralogy & Geochemistry*, **56**(1):1-82. https://doi.org/10.2138/gsrmg.56.1.1

Goulart A.R. 2014. *Geologia e petrografia do picrito do boqueirão e sua correlação com outras rochas máficas ultramáficas no SW do Escudo Sul-riograndense*. Monograph, Instituto de Geociências, Universidade Federal do Rio Grande do Sul, Porto Alegre, 84 p.

Grapes R.H., Hoskin P.W.O. 2004. Epidote Group Minerals in Low–Medium Pressure Metamorphic Terranes. *Reviews in Mineralogy & Geochemistry*, **56**(1):301-345. https://doi.org/10.2138/gsrmg.56.1.301

Grazia C.A., Toniolo J.A., Parisi G., Muller E.L., Dressler V.L. 2011. Prospecção Hidrogeoquímica no Carbonatito Três Estradas, RS. *In*: Congresso Brasileiro de Geoquímica, 13., Gramado. *Annals...*, p. 1769-1772.

Harlov D.E., Austrheim H. (Eds.). 2013. *Metasomatism and the Chemical Transformation of Rock- The Role of Fluids in Terrestrial and Extraterrestrial Processes*. Berlin Heidelberg: Springer-Verlag, 806 p.

Hartmann L.A. 1987. Isócrona Sm-Nd de 2,1 Ga em minerais de duas amostras do Complexo Granulítico Santa Maria Chico, RS. *In*: Congresso Brasileiro de Geoquímica, 1., Porto Alegre. *Anais...*, p. 105-111.

Hartmann L.A. 1991. Condições de Metamorfismo no Complexo Granulítico Santa Maria Chico, RS. *Revista Brasileira de Geociências*, **21**(2):107-113.

Hartmann L.A. 1998. Deepest exposed crust of Brazil- Geochemistry of Paleoproterozoic depleted Santa Maria Chico Granulites. *Gondwana Research*, **1**(3-4):331-341. https://doi.org/10.1016/S1342-937X(05)70849-2

Hartmann L.A., Liu D., Wang Y., Massonne H., Santos J.O.S. 2008. Protolith age of Santa Maria Chico granulites dated on zircons from an associated amphibolite-facies granodiorite in southernmost Brazil. *Anais da Academia Brasileira de Ciências*, **80**(3):543-551. http://dx.doi.org/10.1590/S0001-37652008000300014

Heinrich C.A. 2005. The physical and chemical evolution of low-salinity magmatic fluids at the porphyry to epithermal transition: a thermodynamic study. *Mineralium Deposita*, **39**(8):864-889. http://dx.doi.org/10.1007/s00126-004-0461-9

Henrichs I.A. 2013. *Caracterização e Idade do Sistema Pórfiro Yarumalito, Magmatismo Combia, Colômbia*. Monograph, Instituto de Geociências, Universidade Federal do Rio Grande do Sul, Porto Alegre, 68 p.

Holdaway M.J. 1972. Thermal Stability of Al-Fe Epidote as a Function of fO_2 and Fe Content. *Contributions to Mineralogy and Petrology*, **37**:307-340.

Iglesias C.M.F. 2000. *Análise integrada de dados geológicos e estruturais para a prospecção de ouro na região de Torquato Severo (RS)*. MS Dissertation, Universidade Federal do Rio Grande do Sul, Porto Alegre, 101 p.

Inoue A., Kurokawa K., Hatta T. 2010. Application of Chlorite Geothermometry to Hydrothermal Alteration in Toyoha Geothermal System, Southwestern Hokkaido, Japan. *Resource Geology*, **60**(1):52-70. https://doi.org/10.1111/j.1751-3928.2010.00114.x

Inoue A., Meunier A., Patrier-Mas P., Rigault C., Beaufort D., Viellard P. 2009. Application of chemical geothermometry to low-temperature trioctahedral chlorites. *Clays and Clay Minerals*, **57**(3):371-382. https://doi.org/10.1346/CCMN.2009.0570309

Jiang W.T., Peacor D.R., Buseck P.R. 1994. Chlorite Geothermometry?- Contamination and Apparent Octahedral Vacancies. *Clays and Clay Minerals*, **42**(5):593-605. https://doi.org/10.1346/CCMN.1994.0420512

Jost H., Hartmann L.A. 1984. Província Mantiqueira - Setor Meridional. *In*: Almeida F.F.M., Hasui Y. (Eds.). *O Pré-Cambriano do Brasil*. São Paulo: Edgard Blücher, p. 345-368.

Jowett E.C. 1991. Fitting iron and magnesium into the hydrothermal chlorite geothermometer. *In*: GAC/MAC/SEG Joint Annual Meeting, 16., Toronto. *Annals...*, A62.

Knight C., Bodnar R.J. 1989. Synthetic Fluid Inclusions: Critical PVTX Properties of NaCl-H2O Solutions. *Geochimica et Cosmochimica Acta*, **53**(1):3-8. https://doi.org/10.1016/0016-7037(89)90267-6

Kranidiotis P., MacLean W.H. 1987. Systematics of chlorite alteration at the Phelps Dodge massive sulfide deposit, Matagami, Quebec. *Economic Geology*, 82(7):1898-1911. https://doi.org/10.2113/gsecongeo.82.7.1898

Kühn M. 2004. *Reactive Flow Modeling of Hydrothermal Systems*. Berlin Heidelberg: Springer-Verlag, 261 p.

Laux J.H. 2017. *Geologia e recursos minerais da Folha Lagoa da Meia Lua - SH. 21–Z–B-VI, escala 1:100.000, estado do Rio Grande do Sul*. Porto Alegre: CPRM, 255 p.

Laux J.H., Bongiolo E.M. 2011. Geoquímica do Complexo Granulítico Santa Maria Chico: Arco de Ilha Proterozóico no Rio Grande do Sul. *In*: Congresso Brasileiro de Geoquímica, 13., Gramado. *Anais...*, p. 744-747.

Luzardo R., Fernandes L.A.D. 1990. Análise estrutural do Lineamento de Ibaré Parte I: Filitos de Ibaré - Greenstone Belt ou Cobertura Cratônica Deformada? *Acta Geológica Leopoldensia*, **13**(30):25-36.

Moazzen M. 2004. Chlorite-chloritoid-garnet equilibria and geothermometry in the Sanandaj-Sirjan metamorphic belt, southern Iran. *Iranian Journal of Science & Technology*, Transaction A, **28**(1):65-78. http://dx.doi.org/10.22099/ijsts.2004.2835

Nardi L.V.S., Hartmann L.A. 1979. O Complexo Granulítico Santa Maria Chico do Escudo Sul-riograndense. *Acta Geológica Leopoldensia*, **6**:45-75.

Naumann M.P., Hartmann L.A., Koppe J.C., Chemale Jr. F. 1984. Sequências supra-crustais, gnaisses graníticos, granulitos e granitos intrusivos da região de Ibaré-Palma, RS: geologia, aspectos estratigráficos e considerações geotectônicas. *In*: Congresso Brasileiro de Geologia, 33., Rio de Janeiro. *Anais...*, p. 2417-2425.

Norton D., Knight J. 1977. Transport phenomena in hydrothermal systems: cooling plutons. *American Journal of Science*, **277**(8):937-981. http://dx.doi.org/10.2475/ajs.277.8.937

Panteleyev A. 1996. Epithermal Au-Ag: Low Sulphidation. *In*: Lefebure D.V., Höy T, (Eds.). *Selected British Columbia Mineral Deposit Profiles*. British Columbia: Ministry of Employment and Investment, v. 2, p. 41-44.

Philipp R.P., Gireli T., Lopes R.C., Sander A. 2017. Geologia do Complexo Granulítico Santa Maria Chico na região de Fontouras, Dom Pedrito, RS: significado tectônico e implicações sobre a evolução do Cráton Rio de La Plata, RS, Brasil. *Geologia USP*. (in press).

Phillips G., Hand M., Offler R. 2010. P-T-X controls on phase stability and composition in LTMP metabasite rocks - a thermodynamic evaluation. *Journal of Metamorphic Geology*, **28**(5):459-476. https://doi.org/10.1111/j.1525-1314.2010.00874.x

Pirajno F. 2009. *Hydrothermal Processes and Mineral Systems*. Netherlands: Springer, 1250 p.

Reed M., Rusk B., Palandri J. 2013. The Butte Magmatic-Hydrothermal System: One Fluid Yields All Alteration and Veins. *Economic Geology*, **108**(6):1379-1396. http://dx.doi.org/10.2113/econgeo.108.6.1379

Ribeiro M.J. 1978. *Mapa previsional do cobre no Escudo Sul-Rio-Grandense, escala 1:500.000*. Porto Alegre: DNPM, Seção Geologia Econômica, 104 p.

Roedder E. 1971. Metastability in Fluid Inclusions. *Society of Mining Geology of Japan*, **3**:327-334.

Roedder E. 1984. Fluid Inclusions. *In*: Roedder E. (Ed.). *Review in Mineralogy*. Mineralogy Society of America, v. 12, 644 p.

Rollinson H.R. 1993. *Using geochemical data: evaluation, presentation, interpretation*. Harlow: Longman Scientific & Technical, 352 p.

Ruppel L.M.V. 2010. *Evolução Tectônica do Complexo Arroio da Porteira, Bagé-RS*. Monograph, Instituto de Geociências, Universidade Federal do Rio Grande do Sul, Porto Alegre, 84 p.

Senhorinho E.M. 2012. *Controle Estrutural dos Carbonatitos no Rio Grande do Sul: Análise de Produtos de Sensoriamento Remoto Aerogeofísicos*. Monograph, Instituto de Geociências, Universidade Federal do Rio Grande do Sul, Porto Alegre, 162 p.

701

Shikazono N. 2003. *Geochemical and Tectonic Evolution of Arc-Backarc Hydrothermal Systems- Implication for the Origin of Kuroko and Epithermal Vein-Type Mineralizations and the Global Geochemical Cycle*. Amsterdam: Elsevier Science, 463 p.

Sillitoe R.H. 2015. Epithermal paleosurfaces. *Miner Deposita*, **50**(7):767-793. https://doi.org/10.1007/s00126-015-0614-z

Toniolo J.A., Kirchner C.A. 1995. *Projeto Ouro RS/SC: Área RS-01, Lavras do Sul-Caçapava do Sul - Rio Grande do Sul, escala 1:250.000*. Porto Alegre: CPRM, 1 v. (Informe de Recursos Minerais - Série Mapas Temáticos do Ouro, n. 2, Programa Nacional de Prospecção de Ouro.)

Toniolo J.A., Kirchner C.A. 2000. *Resultados da prospecção para o ouro na área RS-01, Lavras do Sul-Caçapava do Sul, subárea Ibaré - Rio Grande do Sul, escala 1:50.000*. Porto Alegre: CPRM, 1 v. (Informe de Recursos Minerais - Série Ouro, Informes Gerais, n. 8, Programa Nacional de Prospecção de Ouro.)

Toniolo J.A., Remus M.V.D., Parisi G.N., Dani N. 2013. Dois eventos carbonatíticos temporalmente distintos no RS: tipos linear e central. *In*: Simpósio Sul-Brasileiro de Geologia, 8., Porto Alegre. *Anais...*

Vidal O., Parra T., Trotet F. 2001. A thermodynamic model for Fe-Mg aluminous chlorite using data from phase equilibrium experiments and natural pelitic assemblages in the 100° to 600°C, 1 to 25 kb range. *American Journal of Science*, **301**(6):557-592. https://doi.org/10.2475/ajs.301.6.557

Walker J.R. 1993. Chlorite polytype geothermometry. *Clays and Clay Minerals*, **41**(2):260-267. http://www.clays.org/journal/archive/volume%2041/41-2-260.pdf

Walshe J.L. 1986. A six-component chlorite solid solution model and the conditions of chlorite formation in hydrothermal and geothermal systems. *Economic Geology*, **81**(3):681-703. https://doi.org/10.2113/gsecongeo.81.3.681

White N.C., Hedenquist J.W. 1990. Epithermal environments and styles of mineralization: variations and their causes, and guidelines for exploration. *Journal of Geochemical Exploration*, **36**(1-3):445-474. https://doi.org/10.1016/0375-6742(90)90063-G

White N.C., Hedenquist, J.W. 1995. Epithermal gold deposits: styles, characteristics and exploration. *SEG Newsletter*, **23**(1):9-13.

Wildner W., Ramgrab G.E., Lopes R.C., Iglesias C.M.F. 2006. *Mapa Geológico do Estado do Rio Grande do Sul*, escala: 1:750.000. Porto Alegre: Companhia de Pesquisa de Recursos Minerais, Serviço Geológico do Brasil.

Wilkinson J.J. 2001. Fluid inclusions in hydrothermal ore deposits. *Lithos*, **55**(1-4):229-272. https://doi.org/10.1016/S0024-4937(00)00047-5

Winter J.D. 2014. *Principles of Igneous and Metamorphic Petrology*. 2. ed. Harlow: Pearson Education Limited, 738 p.

Yamaguti H.S., Villas R.N. 2003. Estudo microtermométrico dos fluidos hidrotermais relacionados com a mineralização aurífera de Montes Áureos, NW do Maranhão. *Revista Brasileira de Geociências*, **33**(1):21-32.

Yavuz F., Kumral M., Karakaya N., Karakaya M.Ç., Yildirim D.K. 2015. A Windows program for chlorite calculation and classification. *Computers & Geosciences*, **81**:101-113. https://doi.org/10.1016/j.cageo.2015.04.011